Feedbackless Relaying for Enhancing Reliability of Connected Vehicles

G. G. Md. Nawaz Ali, *Member, IEEE*, Beshah Ayalew, *Member, IEEE*, Ardalan Vahidi, *Senior Member, IEEE*, and Md. Noor-A-Rahim

***Abstract*—This paper considers the network- and application-level reliabilities for connected vehicles under path loss environments. We derive a probabilistic framework for estimating reliabilities that is applicable with various path loss models. We also build a realistic connected vehicle traffic simulation environment and use it to perform extensive experiments considering semi-urban traffic. The results show that the achievable reliability performances differ significantly with the path loss models considered. For a moderate communication distance between a transmitter and a receiver, with established deterministic and stochastic path loss models, the network-level reliability is around 55%, whereas with the realistic path loss models that consider obstacles and traffic, the reliability falls below 30%. To improve the network- and application-level reliabilities, we propose a feedbackless relaying mechanism that can be deployed on top of IEEE 802.11p, where, the relay vehicle selection is done autonomously. The relaying mechanism improves the network-level and application-level reliabilities by at least 35% for the studied path loss models.**

***Index Terms*—Vehicular networks, autonomous relaying, reliability, path loss model.**

I. Introduction

THE rapid growth of metropolitan areas has exacerbated traffic congestion and accidents. In the US, the DOT's NHTSA [1] documents roughly 35,000 fatalities and nearly 4 million injuries on roadways on an annual basis and estimates the annual economic loss to exceed $836 billion [2]. In addition, drivers spend billions of unproductive hours waiting in traffic and consume 3.1 billion gallons of fuel every year [3]. Connected and automated vehicle (CAV) technologies are poised to alleviate these economic losses and save lives. USDOT estimates that about 82% of accidents involving unimpaired drivers can be addressed by the successful deployment of connected vehicle (CV) technology [4], [5]. For example, a large percentage (75% from [6]) of vehicular crashes are caused by inattentive/distracted drivers to whom automated control such as emergency braking or pre-emptive warnings and guidance can be delivered via connectivity. Given the ubiquitous connectivity in nearly every aspect of modern society, there are now worldwide efforts from public and private stakeholders to come together and provide vehicles and road-side infrastructure with communication capabilities [7]. Currently there are two trends of research for connected vehicles: DSRC (Dedicated Short Range Communication) [4] and cellular (LTE-V (Long Term Evolution-Vehicle)) also called C-V2X (Cellular-V2X)) [8], [9]. In this paper, we focus on the analysis and improvement of network- and application-level reliabilities of DSRC under realistic propagation loss environments.

DSRC, also known as Wireless Access in Vehicular Environment (WAVE), supports both V2V and V2I communications. WAVE includes IEEE 1609.1 $\sim$ 0.4 standards and SAE J2735 message set dictionary and the emerging J2945.1 communication minimum performance requirement [3]. The periodically broadcast safety messages (also called heartbeat message), such as Cooperative Awareness Message (CAM) [9] or Basic Safety Message (BSM) [4], bears the vehicle's instantaneous maneuvering information, such as location, speed, heading, acceleration, deceleration etc. A vehicle with the on-board Global Navigation Satellite System (GNSS)-based devices (e.g., GPS device), transmits and receives the safety messages. Upon receiving safety messages from neighbor vehicles, using CVSS (Cooperative Vehicle Safety System) application, a vehicle can generate a neighborhood map and warn and display the safe maneuver instructions to the driver audibly/visually.

Although significant resources are being deployed for research and deployment in vehicular networks to date [4], [10], a realistic simulation platform is still of interest due to the high expense of test bed deployment and the need for pre/post analysis of experimental expectations and observations [11], [12]. However, major theoretical and/or simulation-based studies assume the physical layer is perfect or ignore the impact of propagation loss [13]. However, the radio propagation can be interfered by objects such as buildings, buses, or trees and this may deteriorate the claimed communication performance significantly [14]. In urban and suburban environments, two vehicles may have LOS (Light-of-Sight) communication link, NLOS (Non-line-of-sight) communication link (due to intersection-building [15]), or even a (long/heavy commercial) vehicle between two cars may also cause OLOS (Obstructed-LOS) communication [16]. In such common scenarios, the communication performance

Manuscript received October 12, 2019; revised January 30, 2020; accepted March 9, 2020. Date of publication March 16, 2020; date of current version May 14, 2020. This work was supported by the U.S. Department of Energy Vehicle Technologies Office, Project DE-EE0008232. The review of this article was coordinated by Prof. F. Richard Yu. *(Corresponding author: G. G. Md. Nawaz Ali.)*

G. G. Md. Nawaz Ali is with the Department of Applied Computer Science, University of Charleston, Charleston, WV 25304 USA (e-mail: gga@g.clemson.edu).

Beshah Ayalew is with the Department of Automotive Engineering, Clemson University, Clemson, SC 29634 USA (e-mail: beshah@clemson.edu).

Ardalan Vahidi is with the Department of Mechanical Engineering, Clemson University, Clemson, SC 29634 USA (e-mail: avahidi@clemson.edu).

Md. Noor-A-Rahim is with the School of Computer Science and IT, University College Cork, Cork T12 YN60, Ireland (e-mail: m.rahim@cs.ucc.ie).

Digital Object Identifier 10.1109/TVT.2020.2980848

0018-9545 © 2020 IEEE. Personal use is permitted, but republication/redistribution requires IEEE permission.
See https://www.ieee.org/publications/rights/index.html for more information.

Authorized licensed use limited to: UNIVERSITY COLLEGE CORK. Downloaded on March 06,2024 at 19:13:15 UTC from IEEE Xplore. Restrictions apply.

could degrade significantly. In this work, we analyze the impact of obstacles and traffic on the reliability performance of the network for safety message exchanges via V2V.

Though packet delivery ratio (PDR) is a commonly used performance metric (network-level reliability metric) in vehicular network research [17], it does not adequately consider the character of CVSS (Cooperative Vehicular Safety System) applications [18], [19]. CVSS applications have a memoryless property [20]; where the current received packet is enough to provide the updated maneuver information of other vehicles. To measure real-world driver-level experience, application-level performance metrics are often used, such as T-window reliability [20] and application-level latency metric [11]. *For a given transmitter-receiver (Tx-Rx) pair and communication range, T-window reliability can be defined as the probability that at least one packet has been successfully received within a predefined time-frame/window.* This is application dependent. For example, receiving one packet per second from a stopped vehicle may be sufficient for nearby/approaching vehicles to take alternative actions for avoiding a collision. In contrast, for a successful lane changing application, more packets per second may need to be received. In this work, we study both the network- and application-level performances under a realistic vehicular traffic environment. The objective is to analyze the extent of degradation of the application-level reliability under a realistic traffic environment and how to improve it.

There is currently no self-supporting simulator which can perform simulations of the network traffic and CVSS applications together. However, there are efforts to combine different simulators for realizing the V2X (Vehicle-to-Everything) applications [21], [22]. In this work, we have built an integrated simulator environment for analyzing the performance of CVSS applications, including our proposed method for improving their reliability. The developed integrated simulation platform facilitates simulations of the network, realistic traffic and CVSS applications. Our integrated simulator consists of ns-3 (Network Simulator-3) [23] for network simulation, PTV VISSIM for traffic simulation [24], and MATLAB COM (Component Object Model) for facilitating real-time communication between ns-3 and VISSIM through socket API (Application Programming Interface) for performing safety application simulation.

In this paper, we evaluate the performance of CVSS applications under different path loss models. With analytical derivations as well as extensive simulation results, we confirm that both the network-level reliability such as PDR, and application-level reliability such as T-window reliability are not satisfactory at all under LOS/OLOS/NLOS communication loss model. Even under other deterministic loss models, such as Friis-Nakagami, the PDR and T-window reliability are as low as 50% and 70%, respectively. Hence, for mitigating the propagation loss effects, we propose an intelligent deferral based autonomous relaying mechanism for relaying the BSM packet to reach to the furthest vehicles. Existing relaying mechanisms are either acknowledgment based [25]–[27] or only work for a certain geographic area (such as intersection) [15], [17]. However, since IEEE 802.11p based broadcast does not support acknowledgement [4], we propose a relaying mechanism which is feedbackless (that is compatible with IEEE 802.11p) and works both at intersections and straight roads.

In summary, we have the following contributions in this paper,

1) We study the network-level reliability (PDR) and application-level reliability (T-window reliability) for V2V communication in urban/sub-urban environments under different path loss models. This work goes beyond the limited presentation in our recent conference paper [28] where we detail the path loss models and introduce the reliability issues. In particular, in this paper, we derive the analytical expressions for estimating the PDR, T-window reliability, and expected latency.
2) For improving the PDR and reliability, we propose an intelligent autonomous relay selection mechanism which selects the furthest vehicle from the source. The relay vehicle forwards the received BSM. The proposed relaying improves PDR and application-level reliability by at least 35% over the existing IEEE 802.11p technology.
3) We build an integrated simulation environment, which integrates ns-3, PTV VISSIM, and MATLAB COM. We perform an extensive simulation study with the realistic traffic situation in a traffic environment in the neighborhood of CU-ICAR (Clemson University-International Center for Automotive Research) in Greenville, South Carolina, USA.

The rest of the paper is organized as follows. Section II summarizes the related works. Section III describes the system architecture and problem statement. Section IV describes the proposed feedbackless relaying scheme. Section V details the probabilistic analysis of PDR, reliability and expected latency for different loss models. Section VI describes the simulation setup, reliability metrics and performance evaluation. Finally, Section VII presents the conclusions of the paper.

II. Related Works

In the following, we discuss related works in three different categories.

1) Propagation Loss Models: The existing propagation loss models could generally be classified into three groups [29]: i) Abstract propagation loss models, such as Fixed received signal stretch model (regardless of Tx-Rx distance, the received signal power is fixed), and Random propagation loss model (the loss model follows a random distribution) etc.; ii) Deterministic propagation loss models, such as, Friis propagation loss model [30] (calculates quadratic path loss occurring in the free space), Long distance path loss model [16] (calculates the exponential path loss occurring over the Tx-Rx distance) etc.; iii) Stochastic fading models, such as Jakes model [31] (calculates the propagation loss by modeling a set of rays transmitted from a Tx to a Rx via different paths), Nakagami-m model [32] (a special case of Gamma distribution which determines the signal power reception probabilistically dependent on Nakagami model parameters) etc. Mangel *et al.* [15] proposed an NLOS model for road intersections validated by extensive measurements. For modeling the signal attenuation due to buildings, Sommer *et al.* [14] proposed an empirical obstacle shadowing

Authorized licensed use limited to: UNIVERSITY COLLEGE CORK. Downloaded on March 06,2024 at 19:13:15 UTC from IEEE Xplore. Restrictions apply.

model which was verified by extensive measurement results for different types of building obstacles. As an abstract model does not consider Tx-Rx distance and a stochastic fading model does not consider the obstacle geometry, we adopt Friis-Nakagami and LOS/OLOS/NLOS models for comparing the achieved network- and application-level reliabilities.

2) Message Relaying Techniques: A number of works study the message relaying techniques for improving the data dissemination performance. A majority of the existing techniques are acknowledgment based [25]–[27]. Korkmaz *et al.* [25] proposed two IEEE 802.11-based multihop broadcast protocols, called AMB (Ad hoc Multihop Broadcast) and UMB (Urban Multihop Broadcast) for vehicular networks. AMB and UMB work for, respectively, directional broadcast and intersection broadcast. Sahoo *et al.* [26] proposed a binary-partition-based multihop broadcast protocol for disseminating emergency messages in vehicular networks. The focus of the proposed approach is reducing the broadcast delay by minimizing the contention delay in the relay node selection procedure. Cao *et al.* [27] focused on a robust relay selection technique applicable for both general and adverse scenarios. They proposed a distance-based relay selection by incorporating an exponent-based partitioning broadcast protocol and a mini-black-burst-assisted mechanism.

However, as IEEE 802.11p based broadcast does not support acknowledgement [4], a number of works put effort on feedbackless relaying techniques for vehicular networks. Rahim *et al.* [17] showed that at the urban intersection where the communication path between two vehicles is blocked by an urban canyon, mounting an RSU (Road Side Unit) at the intersection-center as a relay node improves the communication performance. Boban *et al.* [33] studied, through real-world experiments, that on highways, LOS between two cars is obstructed by other vehicles around 50% of the time, which reduces the received signal strength by more than 20 dB. They proposed to use an opportunistic tall vehicle(s) for relaying to improve the communication performance. Aygun *et al.* [34] proposed to use a selective relaying technique where only one vehicle will do the relaying for a cluster of vehicles. The clustering formation is adaptive and on the basis of the proximity of the type of the messages to be sent. Some of these ideas inspire the relaying approach we propose in Section IV of this paper.

3) Integrated Traffic, Network, and V2X Application Simulator: There are significant efforts to combine different simulators for realizing V2X (Vehicle-to-Everything) applications. One of the most prominent coupling environments is VSimRTI (V2X Simulation Runtime Infrastructure) to simulate V2X applications and to assess their impacts [21]. Some of the couplings with VSimRTI are SUMO (Simulation of Urban MObility) [12] and JiST (Java in Simulation Time)/SWANS (Scalable Wireless Ad hoc Network Simulator) [35], SUMO and OMNeT++ [36], and MATLAB CCMSim (C2X Channel Model Simulator) and OMNeT++ [21] etc. However, there is no representative interface available in VSimRTI to coupling with PTV VISSIM [37]. Veins platform integrates SUMO and INET framework from OMNeT++ [38]. TraNS (Traffic and Network Simulation Environment (TraNS) combines SUMO and ns-2 (Network Simulator-2) [39], and iTETRIS couples

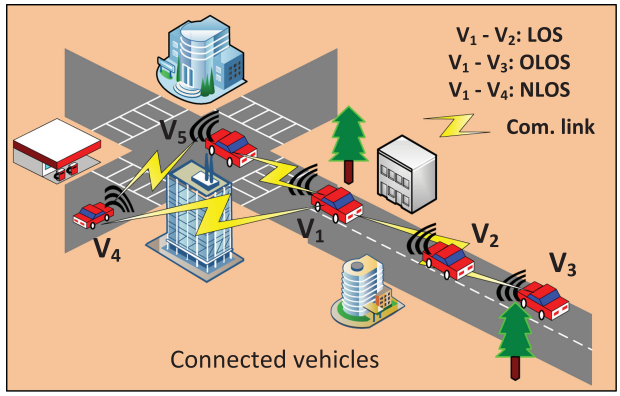

Fig. 1. System architecture.

SUMO and ns-3 (Network Simulator-3) [22]. The development of TraNS and iTETRIS have been ceased and they no longer support the newest version of ns-3. Lochert *et al.* [40] integrates PTV VISSIM [24], MATLAB, and ns-2. However, it lacks information about integrating with ns-3. Note that ns-3 [23] is the newest network simulator and significantly different from ns-2 from various aspects. In this work, we have built an integrated simulation platform that facilitates integrated simulation of the network, realistic traffic, and V2X applications.

III. System Model

A. System Architecture

Fig. 1 shows the typical architecture of connected vehicular networks. We assume a single radio is operating in V2V communication on each vehicle. According to the DSRC multi-channel operation standard, IEEE 1609.4, a vehicle can switch between a control channel (CCH) and one of the six service channels (SCH) [4]. The safety message (BSM) is periodically (at 10 Hz) disseminated through the CCH [17]. Based on the locations of the vehicles and the presence of obstacles, two vehicles could be in LOS (Line-of-sight), OLOS (Obstructed-LOS) or NLOS (Non-LOS) communication links. Hence, based on the type of communication links, the distance between a transmitter and a receiver, and the type of underlying communication loss model, the received signal strength will be different. For instance, in Fig. 1, $V_1 - V_2$ is LOS, while $V_1 - V_3$ (obstructed by V_2) and $V_1 - V_4$ (obstructed by building) are NLOS. We want to study the network-level and application-level reliabilities of CVSS applications under such scenarios.

Referring to Fig. 1, in the straight road scenario, if V_5 cannot receive the signal from V_3 due to the signal attenuation for distance and obstruction (by V_2 and V_1), our proposed autonomous relay selection mechanism (detailed later) will select the relay vehicle V_1. V_1 will relay the BSM of V_3. In the intersection scenario, in the NLOS communication link between V_1 and V_4, V_5 can act as a relay node and exchange the messages between V_1 and V_4. The relay selection mechanism will be discussed in Section IV. The relaying objective is to improve the performance of network-level and application-level reliabilities under realistic path loss conditions.

Authorized licensed use limited to: UNIVERSITY COLLEGE CORK. Downloaded on March 06,2024 at 19:13:15 UTC from IEEE Xplore. Restrictions apply.

B. Problem Statement

In urban/suburban vehicular networks, significant radio signal attenuation might occur due to the distance, multipath signal fading, and shadowing [15] as distance between a transmitter and a receiver vehicles can vary and signals may move through obstacles (e.g., buildings, long and tall vehicles). Communication models that ignore realistic road topologies and obstacles may end up to inconsistent results [41].

For computing the path loss at the receiver, we use the following generalized equation for receive power $P_{Rx}(d)$ at the receiver,

$$P_{Rx}(d) = P_{Tx} + G - \sum PL(d) \tag{1}$$

where, d is the distance between transmitter Tx and receiver Rx; P_{Tx} is the transmit power; G is the antenna gain. $PL(d)$ is the path loss component due to large-scale fading, deterministic obstacle shadowing, and/or of stochastic fast/slow fading.

The value of the path loss component $PL(d)$ varies from one path loss model to another. We have studied a number of path loss models for measuring the path loss effect in semi-urban vehicular traffic [28]. We found that different loss models have different impact on the network- and application-level reliabilites. In particular, the Random loss model has the lowest impact, Friis-Nakagami and long distance have the medium impact, and LOS/OLOS/NLOS model has the highest impact on the reliability performance. For instance, the network- and application-level reliabilities for LOS/OLOS/NLOS model are 30% and 60% for a moderate Tx-Rx distance. These are not satisfactory for safety-critical applications (e.g., CVSS).

Hence, the research question is how to improve both the network- and application-level reliabilities under a realistic path loss setting. To improve the reliability performance, we propose a feedbackless relaying mechanism which improves the reliability by 35% for LOS/OLOS/NLOS model and by 60% for other studied loss models. A brief description of studied path loss models Friis-Nakagami and LOS/OLOS/NLOS is stated in Appendix B. More details can also be found in [28].

IV. Proposed Feedbackless Relaying Technique

For improving the PDR and T-window reliability, we have proposed a relaying mechanism on top of IEEE 802.11p. With the help of a couple of relay vehicles, the overall network performance improves significantly, which is later shown in Figs. 8 and 11 (detailed description is in Section VI).

In our proposed relaying approach, the selection of a relay vehicle is done autonomously by the system. As there is no acknowledgement packet in DSRC based 802.11p, there is neither an RTS (Request to Send)/CTS (Clear to Send) packet nor an RTB (Request to Broadcast)/CTB (Clear to Broadcast) [25], [26] packet to send. But in our approach, the relay vehicle selection is done by a simple feedbackless yet effective method as discussed below.

All the connected vehicles are assumed to obey the rules of IEEE 802.11p transmission rules (Carrier Sense Multiple Access with Collision Avoidance (CSMA/CA)) [4]. However, for relay vehicle selection, we adopt a simple yet effective intelligent defer mechanism on the top of CSMA/CA. When a vehicle receives a BSM in its direction of motion, it will not forward the BSM immediately; rather, it waits for a *ForwardDeferTime*. *ForwardDeferTime* count down starts following a SIFS (Short Inter-frame Space) and it is done independently by each vehicle. While a sending vehicle V_i sends a packet, the *ForwardDeferTime* of a receiving vehicle V_j inside the communication range R of V_i is computed by,

$$DT_{i,j} = \left\lfloor MaxDeferCount \times \frac{(R - \alpha \times d_{i,j})}{R} \right\rfloor \times SlotTime \tag{2}$$

where $0 < \alpha < 1$ is a tuning parameter to give different defer times to vehicles by giving weight to $d_{i,j}$. We set α at 0.5. $d_{i,j}$ is the Minimum Euclidean Distance between V_i and V_j, which is computed by $d_{i,j} = \sqrt{(x_i - x_j)^2 + (y_i - y_j)^2}$, where (x_i, y_i) and (x_j, y_j) are the location coordinates of V_i and V_j, respectively. *MaxDeferCount* is the maximum number of deferred SlotTimes (Typically 20 SlotTimes). A SlotTime is the duration of one slot, which is typically 9 μs. Eq. (2) is computed autonomously by each vehicle. With this computation, the furthest vehicle from the transmitting vehicle will get the shortest defer time, and the closest vehicle will get the longest defer time.

A vehicle V_j, after waiting for $DT_{i,j}$ time, turns around and senses the channel. If it finds the channel is free, it will set the *RelayFlagBit*, add the *RelayVehicleID* on the received BSM packet and rebroadcast after a SIFS time (which is typically 16 μs). On the contrary, if the vehicle finds the channel is busy, which means there is another vehicle further away that is responsible for relaying. Hence, it will discard its *ForwardDeferTime* and returns to the normal Tx/Rx mode. If a vehicle receives a BSM with RelayFlagBit bit set, it will not rebroadcast. In this way, we prevent from rebroadcasting the same packet multiple times.

If a message collision happens (two nodes get the same *ForwardDeferTime*, which is very unlikely), the collision is resolved by a random backoff procedure. The backoff period is chosen randomly from the range of $[0, \frac{DT_{\min}}{2}]$. Note that, in this procedure, only the vehicles whose messages collided will participate. The $DT_{\min}$ is computed by,

$$\begin{aligned} DT_{\min} &= \left\lfloor MaxDeferCount \times \frac{(R - \alpha \times R)}{R} \right\rfloor \times SlotTime \\ &= \lfloor MaxDeferCount \times (1 - \alpha) \rfloor \times SlotTime \end{aligned} \tag{3}$$

In the backoff stage, if the channel is sensed idle for *SlotTime* time period, the counter is decreased by one. The counter will be frozen if the channel is sensed busy. The counter will be resumed once the channel is sensed idle continuously for a SIFS time period. Finally, the packet will be sent as soon as the counter reaches zero. If the collision cannot be resolved by maximum $RET_{\max}$ (<7) times, the relay node selection is discarded with fallback to the normal periodic 802.11p based broadcast. The relay attempts start again at the next broadcast period. Fig. 2(a) shows the sketch of the above described relaying procedure, and Fig. 2(b) shows the modified SAE J2735 DSRC BSM frame part I for relaying, where two additional fields, *RelayVehicleID* and *RelayFlagBit* are inserted.

Authorized licensed use limited to: UNIVERSITY COLLEGE CORK. Downloaded on March 06,2024 at 19:13:15 UTC from IEEE Xplore. Restrictions apply.

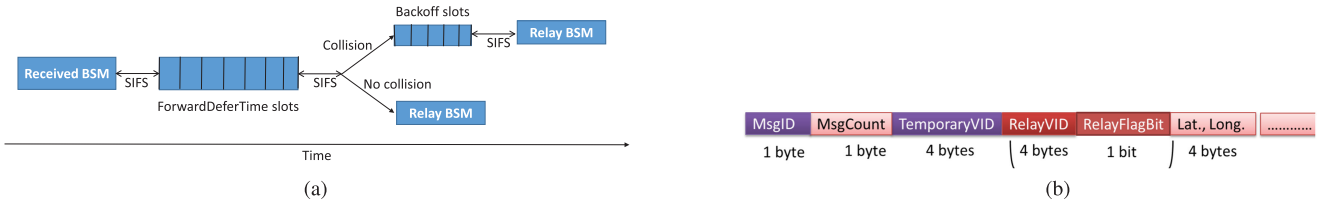

Fig. 2. Relaying mechanism, (a) Relaying procedure, (b) Modified SAE J2735 DSRC BSM frame part I for relaying.

For relay node selection in the intersection case, the *ForwardDeferTime* computation (Eq. (2)) will be updated by the following,

$$DT_{i,c} = \left\lfloor MaxDeferCount \times \frac{R}{(R - \alpha \times d_{i,c})} \right\rfloor \times SlotTime \tag{4}$$

where, $d_{i,c}$ is the Minimum Euclidean Distance between vehicle V_i and the intersection-center (c). In Eq. (4), the vehicle closest to the intersection-center will get the minimum defer time and eventually will be selected as a relay node. The collision resolution backoff time ($DT_{\min}$ (Eq. 3)) will also be updated accordingly. The pseudocode of the proposed relaying mechanism is shown in Appendix A.

V. Probabilistic Analysis

A. Without Relaying

In the following, we demonstrate the probabilistic analysis of PDR, T-window reliability, and EPIL (Expected per-instance latency).

1) Packet Delivery Ratio (PDR): PDR is the average packet delivery ratio for a given communication range. See Section VI-B for a more detailed definition of the PDR. Here, we give expressions for $pdr(d_{\max})$, which is the average packet delivery ratio with maximum <Tx, Rx> distance of $d_{\max}$. We define $pdr(d_{\max})$ by,

$$pdr(d_{\max}) = 1 - \{\mathbb{P}_{Loss}(d_{\max}) + (1 - \mathbb{P}_{Loss}(d_{\max})) \times \mathbb{P}_C\}, \tag{5}$$

The two main components in the PDR calculation are path loss and collision. Here, $\mathbb{P}_{Loss}(d_{\max})$ is the probability of packet loss due to the path loss with distance $d_{\max}$, and $\mathbb{P}_C$ is the probability of packet loss due to packet collision. $\mathbb{P}_C$ depends on the communication range, vehicle density, and transmission rate over the CSMA/CA (Carrier Sense Multiple Access with Collision Avoidance) communication protocol [17], which will be discussed later in this section.

$\mathbb{P}_{Loss}(d_{\max})$ can be computed by,

$$\mathbb{P}_{Loss}(d_{\max}) = \sum_{z=d_{\min}}^{d_{\max}} \Pr(z)\ \mathbf{1}\left(P_{Rx}(z) > \Theta\right) \tag{6}$$

where $d_{\min}$ is the minimum possible distance between <Tx, Rx> and Θ is the receiver sensitivity in dB. In the above equation, $\Pr(z)$ is obtained from the distribution of vehicles along the street and function $\mathbf{1}(P_{Rx}(z) > \Theta)$ returns 1 when $P_{Rx}(z) > \Theta$, otherwise it returns 0.

In the following, we present a semi-analytical method to find $P_{Rx}(z)$, where $P_{Rx}(z)$ is computed by,

$$P_{Rx}(z) = (1 - \mathbb{P}_{Obs}(z)) \times (P_{Tx} + G - PL_X(z)) + \mathbb{P}_{Obs}(z) \times (P_{Tx} + G - PL_X(z) - PL_{NLOS}(z)) \tag{7}$$

where $\mathbb{P}_{Obs}(z)$ is the probability that there are obstacle(s) (for instance buildings) between Tx-Rx provided within the distance z. $PL_{NLOS}(z)$ is the path loss due to the obstacle within Tx-Rx distance z. Both $\mathbb{P}_{Obs}(z)$ and $PL_{NLOS}(z)$ depend on the geography of the region of interest. Numerically one can find $\mathbb{P}_{Obs}(z)$ by curve-fitting on the sample values. $PL_{NLOS}(z)$ can be found from Eq. (25). $PL_X(z)$ is the computed path loss by an underlying path loss model. Note that $PL_X(z)$ for different loss models are described in Appendix B.

Packet collision $\mathbb{P}_C$ can be analyzed as follows. Assume BSM packet generation follows a Poisson distribution with rate r. Hence, the probability that at least one packet is sent by a vehicle V_i in the medium within the average transmission time T_s is,

$$\mathbb{P}_i = 1 - e^{-r.T_s} \tag{8}$$

As in IEEE 802.11p the channel access follows CSMA/CA, where according to [42], the channel access probability of a vehicle V_i is,

$$\tau_i = \frac{1}{\frac{1}{\mathbb{P}_i} + \frac{CW_{\min}+1}{2}} \tag{9}$$

where, $CW_{\min}$ is the minimum contention window size. Assume ρ is the vehicle density (number of vehicles per meter) on the road. Hence, the number of vehicles sharing the same channel of vehicle V_i for communication range R is, $N = 2\rho.R$. With channel access probability τ_i, the probability that vehicle V_i successfully transmits a packet is [43],

$$\mathbb{P}_s^i = \tau_i \times \prod_{j=1}^{N-1} (1 - \tau_i) \tag{10}$$

Hence, the probability that all vehicles successfully transmit a packet is,

$$\mathbb{P}_s = \sum_{i=1}^{N} \mathbb{P}_s^i = \sum_{i=1}^{N} \left(\tau_i \times \prod_{j=1}^{N-1} (1 - \tau_i) \right) \tag{11}$$

The probability that channel is idle, which is equivalent to the probability that none of the vehicles is transmitting, is computed

Authorized licensed use limited to: UNIVERSITY COLLEGE CORK. Downloaded on March 06,2024 at 19:13:15 UTC from IEEE Xplore. Restrictions apply.

by,

$$\mathbb{P}_l = \prod_{i=1}^{N}(1-\tau_i) \tag{12}$$

Hence, the probability of packet collision in the medium is,

$$\begin{aligned}\mathbb{P}_C &= 1 - \mathbb{P}_s - \mathbb{P}_l \\ &= 1 - \sum_{i=1}^{N}\left(\tau_i \times \prod_{j=1}^{N-1}(1-\tau_i)\right) - \prod_{i=1}^{N}(1-\tau_i)\end{aligned} \tag{13}$$

2) T-window Reliability: With the assumption of independent packet drops, the T-window reliability for a maximum Tx-Rx distance of $d_{\max}$ is given by [20],

$$\text{T-window-reliability}(d_{\max}) = 1 - (1 - pdr(d_{\max}))^{\frac{T}{t}}, \tag{14}$$

where t is the BSM generation interval, and T is the duration of tolerance time window, T-window.

3) Expected Per-instance Latency (EPIL): (See Section VI-B for extended definition).

Let T_s be the average time interval from a packet generation to its transmission. Assume, $d_{\max}$ and T are, respectively, the maximum Tx-Rx distance and tolerance time. The expected per-instance latency (EPIL) is given by,

$$\begin{aligned}&\text{EPIL}(d_{\max}, T) \\ &= \sum_{j=1}^{\frac{T}{t}}(T_s + (j-1)t) \times pdr(d_{\max}) \times \{1 - pdr(d_{\max})\}^{j-1} \\ &\quad + \left[1 - \sum_{k=1}^{\frac{T}{t}} pdr(d_{\max})\{1 - pdr(d_{\max})\}^{k-1}\right] \times T\end{aligned} \tag{15}$$

where the first term corresponds to the successful reception of message within time T and the second term corresponds to the event when a message does not get received in time window T.

B. PDR Improvement Through Proposed Relaying Technique

PDR can be improved through relaying. On the top of IEEE 802.11p, using a suitable non-ACK (non-acknowledgment) based relay selection technique, a relay vehicle can be selected in an ad hoc manner. The relay vehicle selection is discussed in Section IV. The relay vehicle can rebroadcast the received message following the CSMA/CA rules. There will be only one relay vehicle inside the communication range R of the original transmitting vehicle. If a vehicle receives a replicated message, it will discard the replicated one. For performing a successful relaying, there should be at least one Tx vehicle inside the range R and at least one Rx vehicle within $2R$ range as shown in Fig. 3. In Fig. 3, while V_1 is the source vehicle, V_3 (not V_2) should be the relay vehicle. In that case, while V_3 rebroadcasts, both V_4 (on the same road) and V_5 (on the cross road) can receive the relayed message.

We assume that the interspaces among vehicles are exponentially distributed. Denoting the average vehicle density by ρ, the probability that a relay vehicle (Tx) and a receiver vehicle (Rx) are within the communication range (R) of each other is,

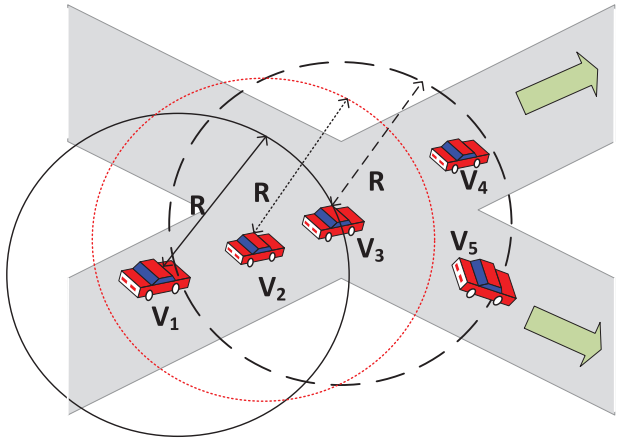

Fig. 3. An instance of relaying.

$$\begin{aligned}\mathbb{P}_{Tx,Rx} &= \mathbb{P}[\text{At least one Tx in } R].\mathbb{P}[\text{At least one Rx in } 2R] \\ &= (1 - e^{-\rho.R}).(1 - e^{-2\rho.R})\end{aligned} \tag{16}$$

The relay vehicle will receive a packet with probability $pdr(d_{\max})$. Hence, with relaying, the probability that a vehicle receives a packet is,

$$\begin{aligned}pdr(relay) &= pdr(d_{\max}) + (1 - pdr(d_{\max})) \\ &\quad \times \{pdr(d_{\max}) \times \mathbb{P}_{Tx,Rx}\} \\ &= pdr(d_{\max}) + (1 - pdr(d_{\max})) \\ &\quad \times \left\{pdr(d_{\max}) \times (1 - e^{-\rho.R}) \times (1 - e^{-2\rho.R})\right\}\end{aligned} \tag{17}$$

Note that $pdr(d_{\max})$ can be computed from (5).

C. Numerical Results

Based on the above described model, to obtain some baseline numerical results of the analytically estimated PDR, T-window reliability, and expected latency, we consider the worst case scenario, where we set $\mathbb{P}_{Obs}(z) = 1$. We assume uniform distribution of vehicles along the streets and we set $\Theta = -85$ dB, $P_{Tx} = 23$ dB, $G = 0$ dB, and $d_{\min} = 1$ m. $PL_{NLOS}(z)$ is calculated from $PL_{NLOS}(z) = 2.331e^{-05}z^3 - 0.005z^2 + 0.517z + 10.67$, which is obtained from the curve-fitting on sample data. For the numerical result of packet collision, we set $T_s = 0.4$ msec, $r = 10$ Hz, $CW_{\min} = 15$ and $\rho = 0.1$ vehicles/m. Fig. 4 shows the comparative numerical results (in terms of PDR, reliability and EPIL) for cases with and without relaying. With the increasing Tx-Rx communication distance for both the Friis-Nakagami and LOS/OLOS/NLOS models, PDRs drop significantly. Note that the LOS/OLOS/NLOS model has the lowest PDR, because the LOS/OLOS/NLOS model considers both the communication distance and the obstacle shadowing. Fig. 4(a) also shows that with addition of a simple relaying technique, PDR improves significantly. With a moderate communication distance (~300 m), the PDR improvement is over 60% for both studied loss models.

Authorized licensed use limited to: UNIVERSITY COLLEGE CORK. Downloaded on March 06,2024 at 19:13:15 UTC from IEEE Xplore. Restrictions apply.

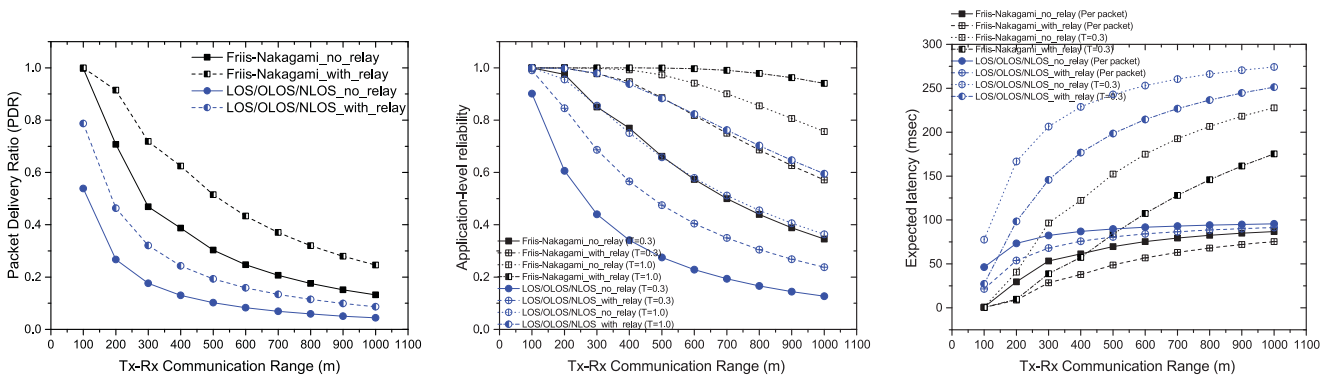

Fig. 4. Numerical results of (a) PDR, (b) T-window reliability, and (c) Expected latency under different path loss models.

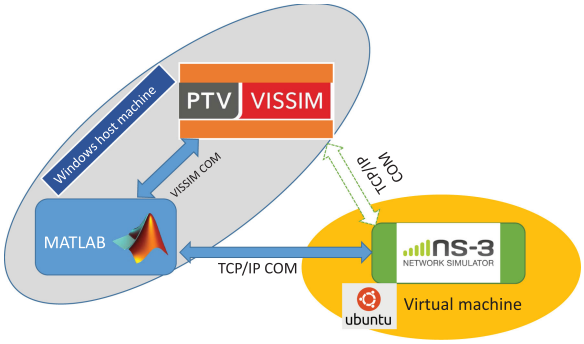

Fig. 5. Simulation setup.

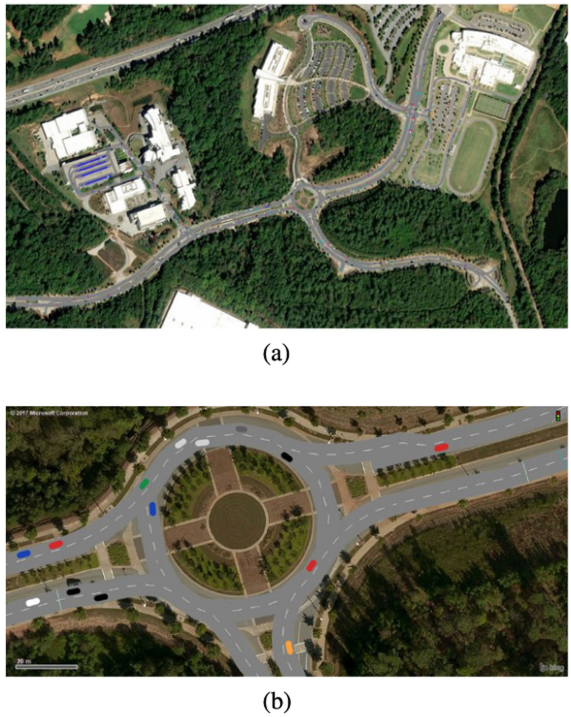

Fig. 6. Vehicular traffic modeling with PTV VISSIM. (a) Simulation area: 1.5 km stretch CU-ICAR neighborhood. (b) A portion of vehicular traffic simulation (Roundabout).

Fig. 4(b) reflects the application-level reliability under different T-window values. With the increasing Tx-Rx communication distance, reliability declines. However, with the different T-window values, a given loss model results in different reliability values. Reliability increases while T-window value increases. With the addition of the proposed relaying technique, the reliability for a loss model for a given T-window value increases by at least 35% with the moderate Tx-Rx communication distances. This shows the efficacy of the proposed relaying technique.

For EPIL (Expected Per-instance Latency) calculation in Eq. ((15)), we set $T_s = 0.4$ msec and $t = 100$ msec. The EPIL result shown in Fig. 4(c) demonstrates that for a loss model, expected per instance latency is much higher than expected per packet latency. Furthermore, in a given T-window, EPIL increases with the increasing Tx-Rx distance. However, note that the maximum EPIL value is lower than the tolerable latency (T-window value). With the proposed relaying technique EPIL is reduced by at least 30%.

VI. Performance Evaluation

A. Simulation Setup

The simulation model is built based on the system architecture described in Section III-A. Fig. 5 shows the integrated simulator, which consists of PTV VISSIM for traffic simulation [24], ns-3 for discrete-event network simulation [23], MATLAB scripting for setting up traffic parameters in VISSIM through VISSIM COM (Component Object Model), and setting real-time communication with ns-3 and VISSIM via TCP/IP socket API.

In every simulation step (100 msec interval), MATLAB sends VISSIM vehicles' position information to ns-3. ns-3 uses the waypoint-mobility-model to create and track the vehicle's position and speed. The different path loss models are incorporated into ns-3. The over 1.5 km long simulation road network is set up consisting the traffic neighborhood of CU-ICAR (Clemson University-International Center for Automotive Research) for simulating realistic traffic as shown in Fig. 6. The simulation network consists of one roundabout, two traffic-light intersections, and two priority intersections. The simulation area also contains buildings, which will be treated as two dimensional

Authorized licensed use limited to: UNIVERSITY COLLEGE CORK. Downloaded on March 06,2024 at 19:13:15 UTC from IEEE Xplore. Restrictions apply.

TABLE I
ns-3 SIMULATION PARAMETERS

Parameter	Value
Number of vehicles	60
Safety message size	200 bytes
Transmission rate	10 Hz
Carrier frequency	5.9 GHz
Channel bandwidth	10 MHz
Data rate	6 Mbps
Transmit power (P_{Tx})	23 dB
Mobility model	Waypoint mobility model
Propagation delay model	Constant speed propagation
Antenna gain (G)	3 dB
VISSIM update rate	0.1 sec

polygonal obstacles for modeling the obstacle shadowing for LOS/OLOS/NLOS loss model. Using the OpenStreetMap [44] the desired test network (.osm file) is extracted which is then passed through the SUMO *polyconvert* utility [12] for extracting the buildings' footprint. The yielded. xml file is then used as input obstacle file in ns-3. For NLOS modeling with the buildings (Eq. (25)), the default α and β values are set to 9 dB and 0.4 dB/m, respectively.

Table I shows the explicit parameters used for VISSIM and ns-3 simulations. The justification for the selection of these values for these parameters can be found in [4], [11], [20], [45]. We follow the DSRC PHY and MAC layers standard [4]. Other than the explicit parameters listed in Table I, other simulation parameters are set at the simulators' default setting.

B. Reliability Metrics

1) Network-Level Reliability: We adopt the following two network-level reliability metrics.

a) Packet delivery ratio (PDR): PDR is a widely accepted network-level reliability metric. For a given range d, the PDR is defined as,

$$pdr(d) = \frac{No.\ of\ actually\ received\ packets}{No.\ of\ expected\ received\ packets} \tag{18}$$

b) Per received packet latency (PRPL): PRPL is the average duration of receiving a packet from its generation. PRPL only considers the received packets in latency calculation.

c) Expected per-packet latency (EPPL): For comparing system performance among the models in terms of latency, considering only successfully received packets is not a fair performance metric [11], hence we consider the latency both for received packets and dropped packets. In terms of a received packet, the latency is the duration from generating a packet to its reception at the receiver. In terms of a dropped packet, latency is equivalent to the packet generation interval. With the 10 Hz broadcast frequency, the lifetime of a packet is 100 msec. Hence, the average expected per-packet latency (EPPL) is,

$$EPPL = \frac{N_{rcv} \times PRPL + N_{drop} \times 100}{N_{rcv} + N_{drop}}$$

where, N_{rcv} is the number of received packets and N_{drop} is the number of dropped packets.

2) Application-Level Reliability: Network-level reliability metrics, alone do not truly measure the driver's (perceived and actual) experience (or in the case of automated vehicles, that of their control system). The sporadic loss of one or two packets may not be experienced by the receiver vehicle, as the recently received packet may be enough to get the updated state of the vehicle. For measuring the application-level reliability we study the following reliability metrics.

a) T-window reliability: It is the probability that at least one packet has been successfully received within a predefined time-frame/window (application dependent). The end user application may not experience any undesired effect, if a receiver vehicle successfully receives at least one packet within the tolerance time-window (T-window). A time instance is called reliable if at least one packet is received within the T-window time, otherwise, that instance is called unreliable. An average T-window reliability of an application is calculated by,

$$\text{T-window-reliability} = \frac{n_{rl}}{n_{rl} + n_{url}}$$

where, n_{rl} is the number of reliable instances and n_{url} is the number of unreliable instances.

The typical CVSS applications based on the tolerable time window (T-window) and the Tx-Rx distance requirement are categorized into several groups [20], [46]. The major CVSS applications fall in the following four categories: SVA (Stop/Slow Vehicle Ahead) advisor, EEBL (Emergency Electronic Brake Light) advisor, FCW (Forward Collision Warning), and LCA (Lane Change & Blind Spot Advisor). In this work, we will maintain a T-window limit in $0.1 \sim 1.0$ sec, and vary the Tx-Rx distance in the range $100 \sim 1000$ m. A lower T-window value means the application is more delay sensitive, such as FCW (typical T-window value is 0.3 sec), on the other hand, a higher T-window value means the application is less delay sensitive, such as SVA (the typical T-window value in such case is 1 sec).

b) Per received instance latency (PRIL): PRIL considers only the reliable instances, which is the average duration of receiving the first successful packet for a given Tx-Rx within a given T-window.

c) Expected per-instance latency (EPIL): EPIL measures the average expected duration from generating a packet to the time the first successful received packet at the receiver for a given Tx-Rx pair within a given T-window. In the EPIL calculation, both reliable and unreliable instances are considered. Hence, the average EPIL is calculated as follows,

$$EPIL = \frac{n_{rl} \times PRIL + n_{url} \times \text{T-window}}{n_{rl} + n_{url}}$$

C. Performance Analysis

In this section, we study the impact of different loss models on the network-level and application-level performance metrics of connected vehicles in urban/sub-urban area. We study the performance of LOS/OLOS/NLOS loss model as a representative of empirical loss models and the Friis-Nakagami as a representative of joint deterministic and stochastic fading models.

Authorized licensed use limited to: UNIVERSITY COLLEGE CORK. Downloaded on March 06,2024 at 19:13:15 UTC from IEEE Xplore. Restrictions apply.

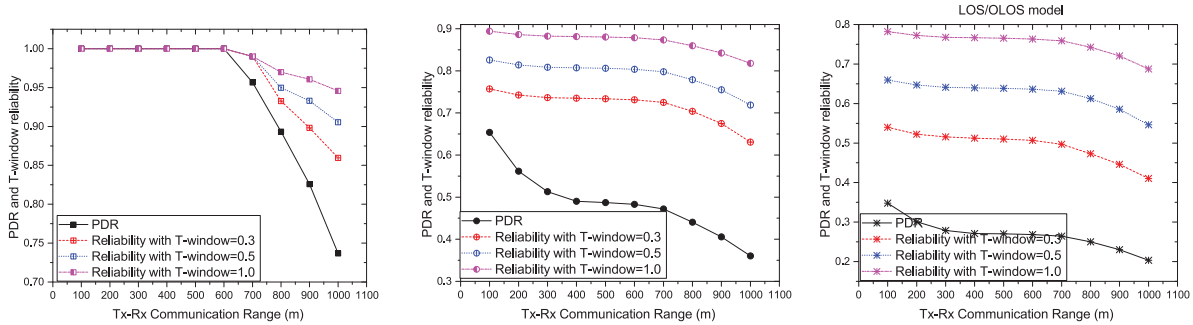

Fig. 7. PDR and T-window reliability with different loss models. (a) No loss model. (b) Friis-Nakagami loss model. (c) LOS/OLOS/NLOS loss model.

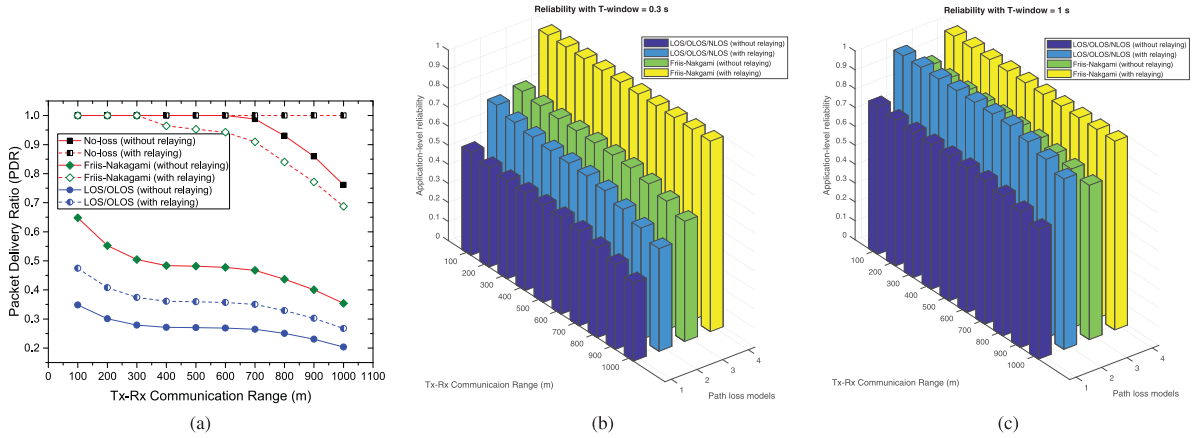

Fig. 8. PDR and reliability improvement through relaying. (a) Packet delivery ratio (PDR). (b) Reliability with T-window = 0.3 sec. (c) Reliability with T-window = 1 sec.

1) Impact on PDR and T-Window Reliability: Fig. 7 exhibits the PDR and the T-window reliability performance under different loss models and no-loss model with different T-window values for varying Tx-Rx communication ranges. As expected, no-loss model has the highest PDR and reliability with different values of T-window (Fig. 7(a)). PDR only starts dropping from 100% when the Tx-Rx communication distance becomes higher than 600 m. The reliability value depends on the T-window value. A higher T-window value results in a higher reliability. When the Tx-Rx communication range equals 1000 m, the reliabilities of the no-loss model are 85%, 90% and 95% for T-window values equal to respectively, 0.3 sec, 0.5 sec, and 1 sec. However, PDRs and reliabilities are significantly lower with the Friis-Nakgami and LOS/OLOS/NLOS models under the increasing Tx-Rx communication ranges. With the moderate communication distance (300 m), PDRs of Friis-Nakagami and LOS/OLOS/NLOS models are around 50% and 30%, respectively. The Friis-Nakgami model has moderate reliability, which is, over 70% with higher T-window values and around 60% with T-window = 0.3 sec. The LOS/OLOS/NLOS model has the lowest reliability. With T-window = 1 sec, the reliability range is 70–80%, whereas, for T-window = 0.5 sec and T-window = 0.3 sec, these ranges are 55–65% and 40–55%, respectively. Hence, with a realistic loss model (such as LOS/OLOS/NLOS), for delay sensitive applications (lower T-window value),

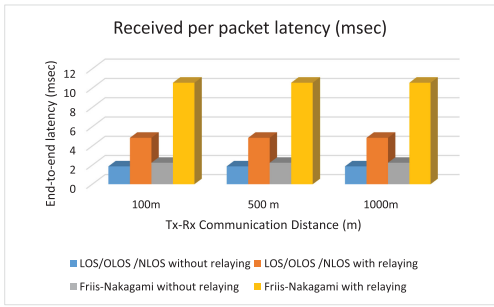

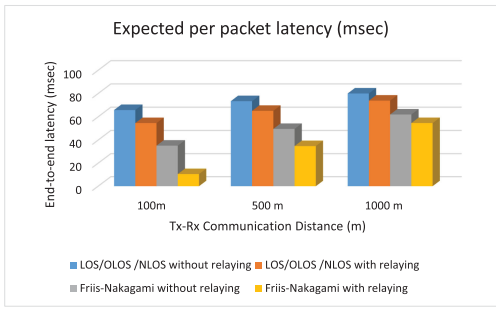

Fig. 9. Latency for per received/expected packet. (a) Per received packet latency. (b) Expected per packet latency.

Authorized licensed use limited to: UNIVERSITY COLLEGE CORK. Downloaded on March 06,2024 at 19:13:15 UTC from IEEE Xplore. Restrictions apply.

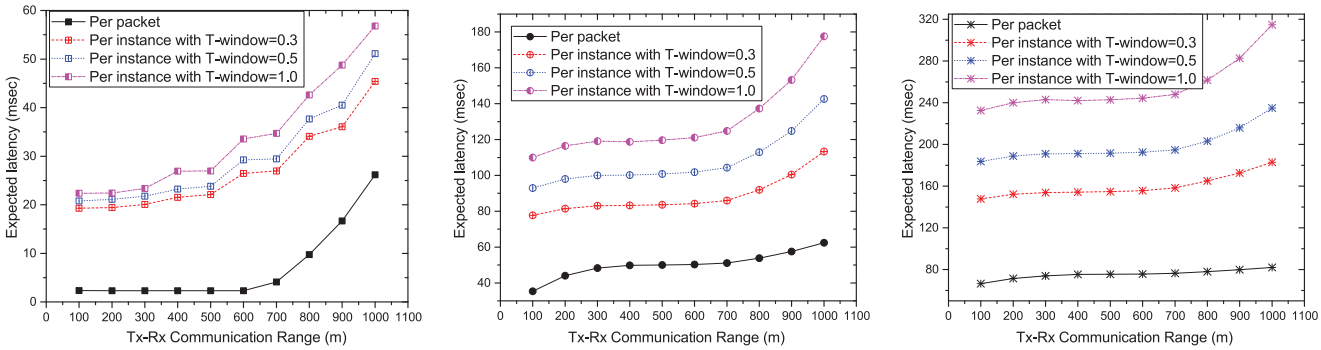

Fig. 10. Expected latency under different loss models. (a) Expected latency with no-loss model. (b) Expected latency with Friis-Nakagami model. (c) Expected latency with LOS/OLOS/NLOS model.

reliability is just over 50% for the communication ranges 100–600 m, which is definitely not a satisfactory performance.

Fig. 8 shows the PDR and reliability improvement through the proposed relaying technique. Fig. 8(a) shows that with the help of relaying, all the studied loss models improve PDR significantly. Depending on the loss model and the Tx-Rx communication distance, these improvements vary from 30% to over 90%. While with the relaying technique, PDR improvement ranges from 30% to 40% for LOS/OLOS/NLOS model under different Tx-Rx communication distance, this improvement is over 50%–90% for the Friis-Nakagami model.

For the reliability improvement, Fig. 8(b) shows that with T-window equal to 0.3 sec, with the help of relaying, the Friis-Nakagami model achieves almost 100% reliability while the LOS/OLOS/NLOS model achieves around 70% reliability. This improvement is around 35% from their no-relaying reliability value. Nevertheless, with T-window = 1 sec, LOS/OLOS/NLOS model also achieves almost 100% reliability even for the Tx-Rx communication distance over 800 m (8c).

2) Impact on Latency: Fig. 9 shows the performance in terms of both per received packet and expected per packet latencies. Fig. 9(a) shows the per received packet latency with and without relaying. Definitely, relaying increases the latency for both the path loss models. Without relaying, per received packet latency (PRPL) is as low as 2 msec. With relaying, PRPL is at most 10 msec. However, interestingly, with relaying, PRPL of Friis-Nakagami model is higher than that of LOS/OLOS/NLOS model. This is because Friis-Nakagami has more received packets (Fig. 8a) than LOS/OLOS/NLOS model. Some late arriving received packets may contribute to higher average latency for Friis-Nakagami model, which could be explained considering the other latency metric, expected per packet latency (EPPL) as shown in Fig. 9(b). In the EPPL calculation for a fair comparison between the path loss models, both the received packets and dropped packets have been considered (Section VI-B1). Hence, if a loss model has more dropped packets, it adds to its EPPL latency. Note that each dropped packet adds 100 msec latency in EPPL calculation. Accordingly, Fig. 9(b) shows that the LOS/OLOS/NLOS model has a higher EPPL than Friis-Nakagami model. Interestingly, it shows that relaying results in a lower EPPL than the case without relaying for both loss models. This is because, relaying has two contradictory impacts on the EPPL. On the one hand relaying improves PDR (8(a)), which reduces the number of dropped packets, hence it impacts positively in reducing EPPL. On the other hand, relaying increases the PRPL for a received packet, which negatively impacts on reducing the EPPL. Hence, it seems the overall EPPL depends on which factor dominates. However, as a dropped packet contributes more latency (100 msec) than a received packet (which is less than 10 msec) in the EPPL calculation, one can conclude that relaying has an overall positive influence for reducing latency in EPPL calculation of a loss model. Nevertheless, the overall EPPL is less than 80 msec, which is less than the packet generation time (100 msec).

Fig. 10 depicts the characteristics of expected per-instance latency (EPIL) and expected per-packet latency (EPPL) of different loss models under various T-window values. Note that although varying the T-window value varies the EPIL of a loss model, it does not affect the EPPL. Hence, EPPL is the same under different T-window values for a given loss model. This is because, EPPL is a network-level performance metric, which is not affected by the application-level parameter, T-window value. Figs. 10(a)–10(c) show that with the increasing communication distance between Tx-Rx, the EPIL increases. This is because, the EPIL calculation considers both the reliable and unreliable instances, and from Fig. 7, with the increasing communication distance reliability declines. This means that with the increasing communication distance, the number of unreliable instances increases. Note that each unreliable instance contributes a T-window equivalence latency in EPIL ($>$100 msec). Fig. 10(a)–10(c) also show that with the increasing T-window value increases the EPIL performance for both path loss models. This is because, with the increasing T-window value, both the tolerable latency for the reliable instances and the dropped latency for the unreliable instances increase. For instance, for T-window = 300 msec, the tolerable latency for reliable instances is $\leq$300 msec and dropped latency for unreliable instance is 300 msec. On the other hand, for T-window = 1 sec, the tolerable latency for reliable instance is $\leq$1 sec and dropped latency for unreliable instance is 1 sec. In summary, the maximum EPPL and EPIL for the no-loss model with a communication range of 1000 m

Authorized licensed use limited to: UNIVERSITY COLLEGE CORK. Downloaded on March 06,2024 at 19:13:15 UTC from IEEE Xplore. Restrictions apply.

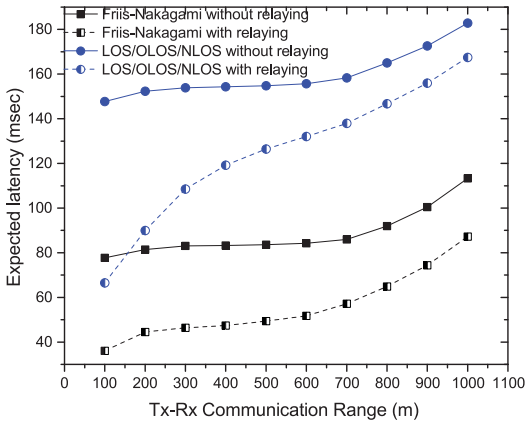

(a)

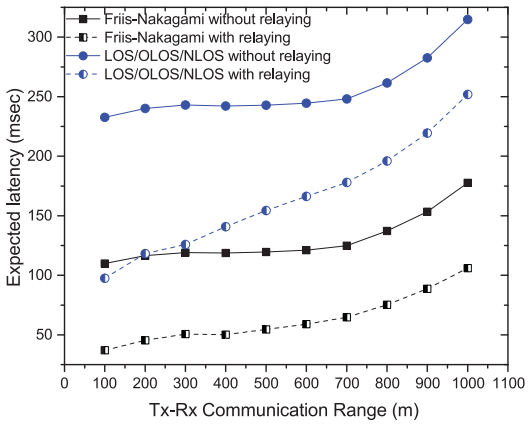

(b)

Fig. 11. Expected latency improvement through relaying. (a) Expected latency for T-window = 300 msec. (b) Expected latency for T-window = 1 sec.

are 28 msec and 57 msec, respectively. Conversely, the highest EPPL and EPIL for the LOS/OLOS/NLOS model are 80 msec (T-window independent) and 315 msec (T-window equals 1 sec), respectively.

Fig. 11 shows the expected per-instance latency (EPIL) improvement through relaying. The proposed relaying technique reduces the EPIL for both loss models significantly. The EPIL reduction for T-window = 0.3 msec, under different communication distances for Friis-Nakagami and LOS/OLOS/NLOS models ranges from 54% to 23% and from to 54% to 9%, respectively. For T-window = 1 sec, this reduction ranges from 66% to 40% and from 58% to 20%, respectively, for Friis-Nakagami and LOS/OLOS/NLOS models. Note that relaying is more effective in EPIL reduction for shorter Tx-Rx communication distances than longer ones. This is because, a shorter communication distance has a higher improved reliability through relaying as shown in Figs. 8(b) and 8(c).

VII. Conclusion and Future Work

In this paper, we have studied the network-level and application-level reliabilities in connected vehicular networks. We have derived probabilistic models for computing network- and application-level reliabilities that can be used with different propagation loss models. For performing a realistic traffic and network simulation, we have also developed an integrated simulator which consists of ns-3, PTV VISSIM, and MATLAB. We have found that there is a significant performance difference between a realistic path loss model such as LOS/OLOS/NLOS and any other existing path loss model. We also found that with a moderate communication distance (300 m) between a Tx-Rx pair, the average network-level and application-level reliabilities with LOS/OLOS/NLOS model are as low as 30% and 60%, respectively. In this paper, we have proposed an autonomous relay selection mechanism that can be deployed on top of IEEE 802.11p. The proposed feedbackless approach selects the furthest vehicle as a relay vehicle and rebroadcasts the received packets to mitigate the signal attenuation effect and delivers the source packet to the furthest vehicles. Our proposed approach improves both the network- and application-level reliabilities by at least 35% for all the studied propagation loss models.

In future work, the plan is to use the calculated network- and application-level reliabilities for dynamically adjusting the broadcasting rate and transmission power for improving PDR (Packet Delivery Ratio) and application-level reliability in (near) real-time.

Appendix A
Feedbackless Relaying Algorithm

Algorithm 1: Feedbackless Relaying Mechanism.

input: Set of vehicles ($\mathbb{V}^i$) inside the communication range of V_i.
output: Relay the received BSM of V_i by identifying relaying vehicle $V_k \in \mathbb{V}^i$.

R is the transmission range of V_i;
Step 1: Compute ForwardDeferTime (DT)
for $\exists V_j \in \mathbb{V}^i$ **do**
  $DT_{i,j} \leftarrow \lfloor MaxDeferCount \times \frac{(R-\alpha \times d_{i,j})}{R} \rfloor \times SlotTime$;
  where,
  $d_{i,j} \leftarrow \sqrt{(x_i - x_j)^2 + (y_i - y_j)^2}$;
  $0 < \alpha < 1$;
  $MaxDeferCount \approx 20\, SlotTimes$;
  $SlotTime \approx 9\, \mu s$;
  Wait for $DT_{i,j}$ duration;
Step 2: Rebroadcast received BSM
/* Find V_k with the minimum ForwardDeferTime (furthest vehicle from V_i) */
Find $V_k \leftarrow V_j \in \mathbb{V}^i$ with the minimum $DT_{i,j}$;
if V_k *finds channel is free* **then**
  Set $RelayFlagBit \leftarrow 1$;
  Add $RelayVehicleID \leftarrow V_k$;
  Rebroadcast BSM after an *SIFS* duration;
/* All other vehicles discard their ForwardDeferTime (DT) */
for $\exists V_j \in \mathbb{V}^i \setminus V_k$ **do**
  Discard $DT_{i,j}$;
  Start sensing channel;
if *a BSM is received with RelayFlagBit* $\equiv$ *1* **then**
  /* The BSM is already been relayed */
  Do not invoke *ForwardDeferTime (DT)* computation;

Authorized licensed use limited to: UNIVERSITY COLLEGE CORK. Downloaded on March 06,2024 at 19:13:15 UTC from IEEE Xplore. Restrictions apply.

APPENDIX B
PATH LOSS MODELS

A brief description of studied loss models is given below.

1) Friis-Nakagami Loss Model: we plug the Nakagami-m [32] fast fading model on the Friis propagation loss model [30] for estimating the realistic loss in the vehicular environment. The Nakagami-m stochastic fading model calculates the small scale fading for the set of rays transmitted in a Tx-Rx pair via different paths. The Nakagami-m fading model, which is a special case of Gamma distribution, determines signal power reception probabilistically dependent on model parameters m and Ω. The PDF is,

$$f(r|m,\Omega) = \frac{2m^m}{\Gamma(m)\Omega^m} r^{2m-1} e^{\{\frac{-mr^2}{\Omega}\}}, r \geq 0 \qquad (19)$$

where m is the Nakagami parameter (i.e., shape parameter with the constraint $m > 1/2$), $\Gamma(m)$ is the gamma function and Ω is the average power of multipath scatter field, which controls the distribution spread, $\Omega = E[r^2]$. When $m = 1$, Nakagami reduces to Rayleigh distribution. For $m > 1$, the fluctuations of the signal strength reduce compared to the Rayleigh fading model, and Nakagami-m tends to Rician fading [47]. The shape parameter m of Nakagami-m is set to 1.5 while Tx-Rx distance is within 80 m, otherwise it is set to 0.75.

Friis propagation loss model calculates the quadratic path loss which occurs in the free space. The path loss in Friis model for Tx-Rx distance d is,

$$PL(d) = 10 \times \log_{10}\left(\left(\frac{4 \times \pi \times d \times f}{c}\right)^2\right) \qquad (20)$$

where, f is the frequency, which is set at 5.9 GHz and c is the speed of light in vacuum (3×10^8 m/s).

2) LOS/OLOS/NLOS Empirical Path Loss Model [11]: computes path losses both for dual slope LOS (Line-of-sight)/OLOS (Obstructed-LOS) path loss model [16] and NLOS (Non-LOS) loss model [14] due to obstacles such as buildings. The path loss for distance d between a Tx and a Rx, due to LOS/OLOS model is [16],

$$PL(d) = \begin{cases} PL(d_0) + 10n_1 \log_{10}\frac{d}{d_0} + X_{\sigma_1}, & \text{if } d \leq d_b \\ PL(d_0) + 10n_1 \log_{10}\frac{d_b}{d_0} + 10n_2 \log_{10}\frac{d}{d_b} + X_{\sigma_2}, & \text{if } d > d_b \end{cases} \qquad (21)$$

where, $PL(d_0)$ is the measured path loss at a reference distance d_0 in dB; d is the distance between Tx and Rx, which is extracted from the received BSM packet. d_b is the breakpoint distance, at what point power decays at different path loss exponent. The fading component, X_σ is a zero-mean Gaussian distributed random variable with standard deviation σ. Distances d_0 and d_b are set at 10 m and 200 m, respectively. The path loss exponents n_1 and n_2 are estimated by linear regression. We use n_1, n_2, X_{σ_1}, X_{σ_2} values fitted from field test data [48].

The overall path loss using LOS/OLOS at receiver of distance d is calculated as follows,

$$PL_{LOS/OLOS}(d) = Prob(LOS|d) \times PL_{LOS}(d) + Prob(OLOS|d) \times PL_{OLOS}(d) \qquad (22)$$

where, $Prob(LOS|d)$ and $Prob(OLOS|d)$ are the probabilities of LOS and OLOS components, respectively. $Prob(LOS|d)$ and $Prob(OLOS|d)$ are calculated using the following empirical equations,

$$Prob(LOS|d) = 1.12e^{-0.0067d} \qquad (23)$$

$$Prob(OLOS|d) = 1 - Prob(LOS|d) \qquad (24)$$

Path loss due to NLOS is computed by [14],

$$PL_{NLOS}(d) = \alpha \times N + \beta \times d_N \qquad (25)$$

where, N counts the number of penetrated walls through the obstacles, and d_N measures the penetrated distance through the obstacles by the drawn ray from Tx to Rx. Coefficients α and β are the attenuation per wall (dB), and the attenuation per meter travel distance (dB/m). α and β values are set based on respectively, type of construction wall (e.g., brick, mortar etc.), and type of buildings (e.g., houses, garages etc.). Hence, the overall path loss captured by the LOS/OLOS/NLOS model is,

$$PL_{LOS/OLOS/NLOS}(d) = PL_{LOS/OLOS}(d) + PL_{NLOS}(d) \qquad (26)$$

REFERENCES

[1] "FARS Encyclopedia," [Online]. Available: http://www-fars.nhtsa.dot.gov/Main/index.aspx. Accessed: Mar. 21, 2020.

[2] K. Abboud, H. A. Omar, and W. Zhuang, "Interworking of DSRC and cellular network technologies for V2X communications: A survey," *IEEE Trans. Veh. Technol.*, vol. 65, no. 12, pp. 9457–9470, Dec. 2016.

[3] G. G. M. N. Ali, M. Noor-A-Rahim, M. A. Rahman, S. K. Samantha, P. H. J. Chong, and Y. L. Guan, "Efficient real-time coding-assisted heterogeneous data access in vehicular networks," *IEEE Internet Things J.*, vol. 5, no. 5, pp. 3499–3512, Oct. 2018.

[4] J. B. Kenney, "Dedicated short-range communications (DSRC) standards in the united states," *Proc. IEEE*, vol. 99, no. 7, pp. 1162–1182, Jul. 2011.

[5] M. Noor-A-Rahim, G. G. M. N. Ali, Y. L. Guan, B. Ayalew, P. H. J. Chong, and D. Pesch, "Broadcast performance analysis and improvements of the LTE-V2V autonomous mode at road intersection," *IEEE Trans. Veh. Technol.*, vol. 68, no. 10, pp. 9359–9369, Oct. 2019.

[6] "The Intelligent Vehicle Initiative." [Online]. Available: https://www.fhwa.dot.gov/. Accessed: Mar. 21, 2020.

[7] J. Guo, B. Song, Y. He, F. R. Yu, and M. Sookhak, "A survey on compressed sensing in vehicular infotainment systems," *IEEE Commun. Surv. Tut.*, vol. 19, no. 4, pp. 2662–2680, Oct.-Nov. 2017.

[8] J. Du, F. R. Yu, X. Chu, J. Feng, and G. Lu, "Computation offloading and resource allocation in vehicular networks based on dual-side cost minimization," *IEEE Trans. Veh. Technol.*, vol. 68, no. 2, pp. 1079–1092, Feb. 2019.

[9] A. Bazzi, B. M. Masini, A. Zanella, and I. Thibault, "On the performance of ieee 802.11p and LTE-V2V for the cooperative awareness of connected vehicles," *IEEE Trans. Veh. Technol.*, vol. 66, no. 11, pp. 10 419–10 432, Nov. 2017.

[10] "U.S. Department of Transportation." [Online]. Available: https://www.transportation.gov/. Accessed: Mar. 21, 2020.

[11] G. G. M. N. Ali, M. Noor-A-Rahim, P. H. J. Chong, and Y. L. Guan, "Analysis and improvement of reliability through coding for safety message broadcasting in urban vehicular networks," *IEEE Trans. Veh. Technol.*, vol. 67, no. 8, pp. 6774–6787, Aug. 2018.

[12] "Simulation of Urban MObility (SUMO)," [Online]. Available: http://sumo.dlr.de/. Accessed: Mar. 21, 2020.

Authorized licensed use limited to: UNIVERSITY COLLEGE CORK. Downloaded on March 06,2024 at 19:13:15 UTC from IEEE Xplore. Restrictions apply.

[13] K. Liu, J. Ng, V. Lee, S. Son, and I. Stojmenovic, "Cooperative data scheduling in hybrid vehicular Ad hoc networks: VANET as a software defined network," *Netw., IEEE/ACM Trans.*, vol. 24, no. 3, pp. 1759–1773, Jun. 2016.
[14] C. Sommer, D. Eckhoff, R. German, and F. Dressler, "A computationally inexpensive empirical model of IEEE 802.11p radio shadowing in urban environments," in *Proc. 8 Int. Conf. Wireless On-Demand Netw. Syst. Serv.*, 2011, pp. 84–90.
[15] T. Mangel, O. Klemp, and H. Hartenstein, "5.9 GHz inter-vehicle communication at intersections: A validated non-line-of-sight path-loss and fading model," *EURASIP J. Wireless Commun. Netw.*, vol. 2011, no. 1, 2011, Art. no. 182.
[16] J. K. T. Abbas, K. Sjberg, and F. Tufvesson, "A measurement based shadow fading model for vehicle-to-vehicle network simulations," *Int. J. Antennas Propag.*, 2015, pp. 1–12, Art. no. 190607.
[17] M. Noor-A-Rahim, G. G. M. N. Ali, H. Nguyen, and Y. L. Guan, "Performance analysis of IEEE 802.11p safety message broadcast with and without relaying at road intersection," *IEEE Access*, vol. 6, pp. 23 786–23 799, 2018.
[18] M. Sookhak *et al.*, "Fog vehicular computing: Augmentation of fog computing using vehicular cloud computing," *IEEE Veh. Technol. Mag.*, vol. 12, no. 3, pp. 55–64, Sep. 2017.
[19] F. Zhang, Y. Du, W. Liu, and P. Li, "Model predictive power control for cooperative vehicle safety systems," *IEEE Access*, vol. 6, pp. 4797–4810, 2018.
[20] F. Bai and H. Krishnan, "Reliability analysis of DSRC wireless communication for vehicle safety applications," in *Proc. IEEE Intell. Transp. Syst. Conf.*, Sep. 2006, pp. 355–362.
[21] R. Protzmann, K. Mahler, K. Oltmann, and I. Radusch, "Extending the V2X simulation environment vsimrti with advanced communication models," in *Proc. 12th Int. Conf. ITS Telecommun.*, Nov. 2012, pp. 683–688.
[22] "iTETRIS: The Open Simulation Platform for Intelligent Transport System (ITS) Services," [Online]. Available: http://www.ict-itetris.eu/. Accessed: Mar. 21, 2020.
[23] "ns-3: A Discrete-Event Network Simulator," [Online]. Available: https://www.nsnam.org/. Accessed: Mar. 21, 2020.
[24] "PTV VISSIM," [Online]. Available: https://www.ptvgroup.com/en/solutions/products/ptv-vissim/. Accessed: Mar. 21, 2020.
[25] G. Korkmaz, E. Ekici, and F. Ozguner, "Black-burst-based multihop broadcast protocols for vehicular networks," *IEEE Trans. Veh. Technol.*, vol. 56, no. 5, pp. 3159–3167, Sep. 2007.
[26] J. Sahoo, E. H. Wu, P. K. Sahu, and M. Gerla, "Binary-partition-assisted MAC-layer broadcast for emergency message dissemination in VANETs," *IEEE Trans. Intell. Transp. Syst.*, vol. 12, no. 3, pp. 757–770, Sep. 2011.
[27] D. Cao, B. Zheng, B. Ji, Z. Lei, and C. Feng, "A robust distance-based relay selection for message dissemination in vehicular network," *Wireless Netw.*, vol. 26, pp. 1755–1771, Oct. 2018.
[28] G. G. M. N. Ali, B. Ayalew, A. Vahidi, and M. Noor-A-Rahim, "Analysis of reliabilities under different path loss models in urban/sub-urban vehicular networks," in *Proc. IEEE 90th Veh. Technol. Conf.*, Sep. 2019, pp. 1–6.
[29] M. Stoffers and G. Riley, "Comparing the ns-3 propagation models," in *Proc. IEEE 20th Int. Symp. Model., Anal. Simul. Comput. Telecommun. Syst.*, Aug. 2012, pp. 61–67.
[30] H. T. Friis, "A note on a simple transmission formula," *Proc. IRE*, vol. 34, no. 5, pp. 254–256, May 1946.
[31] Y. R. Zheng and C. Xiao, "Simulation models with correct statistical properties for rayleigh fading channels," *IEEE Trans. Commun.*, vol. 51, no. 6, pp. 920–928, Jun. 2003.
[32] M. Nakagami, "The m-distributiona general formula of intensity distribution of rapid fading," in *Stat. Methods in Radio Wave Propag.*, W. Hoffman, Ed. New York, NY, USA: Pergamon, 1960, pp. 3–36.
[33] M. Boban, R. Meireles, J. Barros, P. Steenkiste, and O. K. Tonguz, "TVR–Tall vehicle relaying in vehicular networks," *IEEE Trans. Mobile Comput.*, vol. 13, no. 5, pp. 1118–1131, May 2014.
[34] B. Aygun, C. Lin, S. Shiraishi, and A. M. Wyglinski, "Selective message relaying for multi-hopping vehicular networks," in *Proc. IEEE Veh. Netw. Conf.*, Dec. 2016, pp. 1–8.
[35] "JiST/SWANS: Java in Simulation Time/Scalable Wireless Ad hoc Network Simulator," [Online]. Available: http://jist.ece.cornell.edu/sw.html. Accessed: Mar. 21, 2020.
[36] N. Goebel, R. Bialon, M. Mauve, and K. Graffi, "Coupled simulation of mobile cellular networks, road traffic and V2X applications using traces," in *Proc. IEEE Int. Conf. Commun.*, May 2016, pp. 1–7.
[37] A. Choudhury, T. Maszczyk, C. B. Math, H. Li, and J. Dauwels, "An integrated simulation environment for testing V2X protocols and applications," *Procedia Comput. Sci.*, vol. 80, pp. 2042–2052, 2016.
[38] H. Noori, "Realistic urban traffic simulation as vehicular ad-hoc network (VANET) via veins framework," in *Proc. 12th Conf. Open Innov. Assoc.*, Nov. 2012, pp. 1–7.
[39] M. Piórkowski, M. Raya, A. L. Lugo, P. Papadimitratos, M. Grossglauser, and J.-P. Hubaux, "Trans: Realistic joint traffic and network simulator for vanets," *SIGMOBILE Mob. Comput. Commun. Rev.*, vol. 12, no. 1, pp. 31–33, Jan. 2008.
[40] C. Lochert, A. Barthels, A. Cervantes, M. Mauve, and M. Caliskan, "Multiple simulator interlinking environment for ivc," in *Proc. 2nd ACM Int. Workshop Veh. Ad Hoc Netw.*, 2005, pp. 87–88.
[41] F. J. Martinez, M. Fogue, C. K. Toh, J.-C. Cano, C. T. Calafate, and P. Manzoni, "Computer simulations of VANETs using realistic city topologies," *Wireless Pers. Commun.*, vol. 69, no. 2, pp. 639–663, 2013.
[42] Y. P. Fallah, C. Huang, R. Sengupta, and H. Krishnan, "Analysis of information dissemination in vehicular Ad-hoc networks with application to cooperative vehicle safety systems," *IEEE Trans. Veh. Technol.*, vol. 60, no. 1, pp. 233–247, Jan. 2011.
[43] F. Zhang, G. Tan, C. Yu, N. Ding, C. Song, and M. Liu, "Fair transmission rate adjustment in cooperative vehicle safety systems based on multi-agent model predictive control," *IEEE Trans. Veh. Technol.*, vol. 66, no. 7, pp. 6115–6129, Jul. 2017.
[44] "OpenStreetMap." [Online]. Available: https://www.openstreetmap.org/. Accessed: Mar. 21, 2020.
[45] G. N. Ali, P. H. J. Chong, S. K. Samantha, and E. Chan, "Efficient data dissemination in cooperative multi-RSU Vehicular Ad Hoc Networks (VANETs)," *J. Syst. Softw.*, vol. 117, pp. 508–527, 2016.
[46] X. Yin, X. Ma, K. S. Trivedi, and A. Vinel, "Performance and reliability evaluation of BSM broadcasting in DSRC with multi-channel schemes," *IEEE Trans. Comput.*, vol. 63, no. 12, pp. 3101–3113, Dec. 2014.
[47] I. Souid, H. B. Chikha, and R. Attia, "Blind spectrum sensing in cognitive vehicular Ad hoc networks over nakagami-m fading channels," in *Proc. Int. Conf. Elect. Sci. Technol. Maghreb*, Nov. 2014, pp. 1–5.
[48] "Smart Mobility Test Bed (SMTB), NTU, Singapore," [Online]. Available: http://www.infinitus.eee.ntu.edu.sg/Programmes/SMP/Pages/home.aspx. Accessed: Mar. 21, 2020.

G. G. Md. Nawaz Ali (Member, IEEE) received the B.Sc. degree in computer science and engineering from the Khulna University of Engineering & Technology, Khulna, Bangladesh, in 2006, and the Ph.D. degree in computer science from the City University of Hong Kong, Hong Kong, in 2013. He is currently working as an Assistant Professor with the Department of Applied Computer Science, University of Charleston (UC), Charleston, WV, USA. Prior to joining UCWV, he was a Postdoctoral Fellow with the Department of Automotive Engineering, the Clemson University International Center for Automotive Research, Greenville, SC, USA from March 2018 to July 2019. From October 2015 to March 2018, he was a Postdoctoral Research Fellow with the School of Electrical and Electronic Engineering of Nanyang Technological University, Singapore. His current research interests include vehicular cyber physical system, wireless broadcasting, mobile computing, and network coding. He receives the Outstanding Academic Performance Award, from the City University of Hong Kong.

Authorized licensed use limited to: UNIVERSITY COLLEGE CORK. Downloaded on March 06,2024 at 19:13:15 UTC from IEEE Xplore. Restrictions apply.

Beshah Ayalew (Member, IEEE) received the M.S. and Ph.D. degrees in mechanical engineering from Penn State University, State College, PA, USA, in 2000 and 2005, respectively. He is a CECAS Dean's Distinguished Professor of Automotive Engineering with the Clemson University-International Center for Automotive Research, Greenville, SC, USA. He has authored/co-authored more than 150 refereed publications. His interest and expertise are in controls and dynamical systems with applications in connected and automated vehicle traffic systems and energy systems. Dr. Ayalew has been elected fellow of the American Society of Mechanical Engineers (ASME) (2018) for contributions to his field. He is a member of ASME and SAE. He was the recipient of the Ralph R. Teetor Educational Award from the Society of Automotive Engineers (SAE) International (2014), the Clemson University Board of Trustees Award for Faculty Excellence (2012, 2019), and the National Science Foundation's CAREER Award (2011). He was also the recipient of the Penn State Alumni Association Dissertation Award (2005). He currently serves as an Associate Editor for the IEEE TRANSACTIONS ON INTELLIGENT TRANSPORTATION SYSTEMS.

Ardalan Vahidi (Senior Member, IEEE) received the B.S. and M.Sc. degree from Sharif University, Tehran, Iran in 1996 and 1998, respectively, the M.Sc. degree in transportation safety from George Washington University, Washington, DC, USA, in 2002, and the Ph.D. degree in mechanical engineering from the University of Michigan, Ann Arbor, MI, USA, in 2005. He is a Professor of Mechanical Engineering with Clemson University, Clemson, SC, USA. In 2012–2013, he was a Visiting Scholar with the University of California, Berkeley. He has also held scientific visiting positions with BMW Technology Office in California, and with IFP Energies Nouvelles, in France. His research interests include intersection of energy, vehicular systems, and automatic control. He has led a number of projects demonstrating successful implementation of advanced control methods on connected and automated vehicles increasing energy efficiency.

Md. Noor-A-Rahim received the Ph.D. degree from the Institute for Telecommunications Research, University of South Australia, Adelaide, SA, Australia, in 2015. He was a Postdoctoral Research Fellow with the Centre for Infocomm Technology, Nanyang Technological University, Singapore. He is currently a Senior Postdoctoral Researcher (MSCA Fellow) with the School of Computer Science & IT, University College Cork, Cork, Ireland. His research interests include control over wireless networks, intelligent transportation systems, information theory, signal processing, machine learning, and DNA-based data storage. He was the recipient of the Michael Miller Medal from the Institute for Telecommunications Research, University of South Australia, for the most outstanding Ph.D. thesis in 2015.

Authorized licensed use limited to: UNIVERSITY COLLEGE CORK. Downloaded on March 06,2024 at 19:13:15 UTC from IEEE Xplore. Restrictions apply.